

# Evolution of the surface magnetic field of rotating proto-neutron stars

M Obergaulinger and M<sup>Á</sup> Aloy

Departamento de Astronomía y Astrofísica, Universidad de Valencia, C/ Dr. Moliner 50, 46100 Burjassot, Spain

E-mail: martin.obergaulinger@uv.es

**Abstract.** We study the evolution of the field on the surface of proto-neutron stars in the immediate aftermath of stellar core collapse by analyzing the results of self-consistent, axisymmetric simulations of the cores of rapidly rotating high-mass stars. To this end, we compare the field topology and the angular spectra of the poloidal and toroidal field components over a time of about one seconds for cores. Both components are characterized by a complex geometry with high power at intermediate angular scales. The structure is mostly the result of the accretion of magnetic flux embedded in the matter falling through the turbulent post-shock layer onto the PNS. Our results may help to guide further studies of the long-term magnetothermal evolution of proto-neutron stars. We find that the accretion of stellar progenitor layers endowed with low or null magnetization bury the magnetic field on the PNS surface very effectively.

## 1. Introduction

The wide range of surface magnetic field strengths found across the population of neutron stars (e.g. [5]) is the result of a combination of processes operating at their formation during stellar core collapse and effects that modify their structure afterwards, such as cooling or accretion. Most observations pertain to relatively old neutron stars, and do not place tight constraints on the very early evolution of the field. Hence, it is difficult to draw conclusions on the fields of nascent proto-neutron stars (PNSs) from observations or, conversely, to connect theoretical results from models of supernova core collapse to evolved neutron stars. Nevertheless, the field is likely to bear at least a significant imprint of these early conditions.

A thorough theoretical study of the evolution of the magnetic field of PNSs should optimally be based on three-dimensional long-term simulations including magnetohydrodynamics and neutrino transport, which treat the global dynamics of core collapse and a possible supernova explosion and the generation of the PNS field in a self-consistent manner. The enormous computational costs of spectral neutrino transport mean that thus far only a small number of such simulations exist with the most sophisticated ones [17, 7, 6] run for only a fairly limited period.

Hence, less expensive axisymmetric models are still of considerable use for approaching this topic (e.g. [2, 1, 15, 3, 11]). Depending on the rotational energy and the seed field of the pre-collapse star, but also potentially on the input physics and the numerical method and grid resolution, their results range from minor modifications of non-magnetized versions of the same cores to magnetically driven explosions of a preferentially axial morphology. Depending on the

global evolution, the PNS may accrete matter at all latitudes or only through narrow streams with a potential final collapse to a black hole (BH). The time evolution of the rate and geometry of mass accretion and the magnetization of the accreted layers have an important impact on the accumulation of magnetic flux at the PNS surface. The picture thus generated may show a shell of enhanced magnetic field strength, but it is also possible for the magnetic field to be buried underneath additional layers of weakly magnetized gas [16]. These processes are complemented by the possible amplification of magnetic fields in the interior of the PNS, in particular if rotation and convection constitute a dynamo.

Previously, we studied the evolution of magnetized core collapse for stars with an initial mass of  $15 M_{\odot}$  without rotation [9]. Varying the pre-collapse field strength between negligible values below  $10^{10}$  G and dynamically relevant, yet from the point of view of stellar evolution rather overestimated, values of  $10^{12}$  G, we found explosions driven by neutrino heating with potentially a strong contribution of magnetic forces. We were following the evolution of the PNSs for several hundreds of milliseconds and found the development of layers of strong field on their surfaces owing their origin to the accretion of magnetized gas. We now focus on cores of higher-mass stars with rapid rotation and study the geometry of the magnetic field during the first up to two seconds after PNS formation [8]. We note that our set of models includes both PNSs that collapse to a BH within this time and ones that will likely remain stable for much longer or potentially indefinitely.

We outline our simulations in Sect. 2, discuss the result in Sect. 3, and present our conclusions in Sect. 4.

## 2. Simulations

Our numerical models of the stellar cores are based on special relativistic magnetohydrodynamics (MHD), an approximately general relativistic gravitational potential, and spectral neutrino transport. Neutrino physics is treated in the hyperbolic two-moment formulation, which provides a good approximation to a full solution of the Boltzmann equation of radiative transfer and is intrinsically multi-dimensional, and includes corrections due to the gas velocity (e.g., Doppler shifts) and gravity and all relevant interactions between neutrinos of all flavours and nucleons, nuclei, and electrons and positrons [4]. The transport solver, computationally the most expensive part of the simulations, is the main factor restricting us to axisymmetric rather than full three-dimensional simulations.

As reported in [8], we simulated the core collapse of several stars with a high initial mass of  $35 M_{\odot}$  and subsolar metallicity (pre-collapse models 350B and 350C of [18]). To test whether these properties make them viable progenitors of long GRBs, we combined the progenitors with different rotational profiles and magnetic fields. The results can be briefly summarized as follows:

- In spite of their high compactness, usually taken as an indication for a high resistance to shock revival [10], our cores develop successful supernova explosions predominantly driven either by neutrino heating or by magnetorotational stresses. All explosions have a bipolar geometry with the magnetically driven showing the highest degree of collimation of the ejecta and the highest explosion energies.
- While the ejecta expand asymmetrically, matter continues to fall onto the PNS, which therefore grows in mass. For most of our models, the PNS reaches the threshold for BH formation within less than 2 s after bounce. Some models within this class show conditions that make a later collapsar phase conceivable.
- Models without a BH collapse tend to contain a rapidly rotating and hence notably flattened PNS of relatively strong magnetization.

In the following, we will present a study of the magnetic fields on the surfaces of the PNSs of a selection of cores. We focus on both models that collapse to BHs and models where the

PNS remains stable throughout the simulation. Although the simulations end too early for observing the crust formation [13] and the late time fall back of magnetized gas [16], we intend to get insights on the field structure of the very young neutron stars. To this end, we focus on the time evolution of the strengths of the poloidal and toroidal components of the surface field and analyze their multipole expansion in spherical harmonics in order to distinguish large-scale structures from the field fluctuating on small scales. We refer to Fig. 1 for the pre-collapse state of the models, which, as the blue lines indicate, all rotate rapidly and differentially. We briefly describe their dynamics in the following:

**Model 350C-R0** includes the original rotational profile and magnetic field distribution of the core as given by the stellar evolution models. The field has roughly similarly strong poloidal and toroidal components and is confined to the radiative zones of the core. About 200 ms after core bounce, the model develops an explosion driven by a combination of magnetic forces and neutrino heating. The ejecta expand in the form of bipolar outflows along the rotational axis while matter falls onto the PNS, whose mass and rotational energy continue to grow. The accretion, however, does not reach the threshold of collapse to a BH.

**Model 350C-Rs** has a strong initial magnetic field based on the vector potential of [14] with the normalization set such that the profiles of toroidal and poloidal are equal and launches a magnetically powered, very energetic explosion almost immediately after bounce. The explosion quenches the accretion onto the PNS rather effectively, leading to a reduced PNS mass and possibly preventing BH formation indefinitely. Internal redistribution of angular momentum from the centre to the outer layers makes the PNS assume an extremely oblate shape.

**Model 350B-R0** has the much weaker and strongly toroidally dominated magnetic field of the progenitor star 350B, mostly eliminating the magnetic contribution to shock revival. The higher compactness of the pre-collapse core causes the PNS to exceed the instability threshold and collapse to a BH at  $t \sim 1.5$  s.

The magnetic field distribution of the stellar evolution models 350B/C is the result of a simple model for the amplification of the field by a dynamo operating only in radiative zones of the stars [12]. The cores do not include any magnetic field in convective zones. Consequently, there are large field-free regions in the cores, of which the ones outside the iron core of model 350B are of particular importance, as we will show below.

### 3. Results

We illustrate the evolution of the surface field of the three models in Fig. 2. At three selected times between an early stage after bounce and one late in the evolution (close to BH collapse for model 350B-R0), we identified the PNS surface with the angle-dependent radius of  $\nu_e$ -sphere,  $R_\nu(\theta)$  and focussed on a region centred at this radius,  $r(\theta) \in [R_{\min}; R_{\max}] = [R_\nu(\theta) - \Delta R; R_\nu(\theta) + \Delta R]$  with  $\Delta R = 4$  km. The top row of the figure shows the current density,  $j = (\vec{\nabla} \times \vec{b})^\phi$ , and the toroidal field strength together with (poloidal) field lines in this region. Since the radii of the PNS surface decreases as time progresses, the three areas in each panel possess an ordering in time with the outermost and innermost being the first and last of the three times, respectively. In addition, we computed the angular spectra of the field at the same times (bottom row of panels) by expanding its volume-averaged poloidal and toroidal components in terms of spherical harmonics  $Y_{lm}$  ( $m = 0$  because of axisymmetry):

$$b_l^{\text{pol},\phi} = \int d\theta Y_{lm}(\theta) \tilde{b}^{\text{pol},\phi}(\theta), \quad (1)$$

$$\tilde{b}^{\text{pol},\phi}(\theta) = \int dV b^{\text{pol},\phi}(r, \theta) \left( \int dV \right)^{-1}, \quad (2)$$

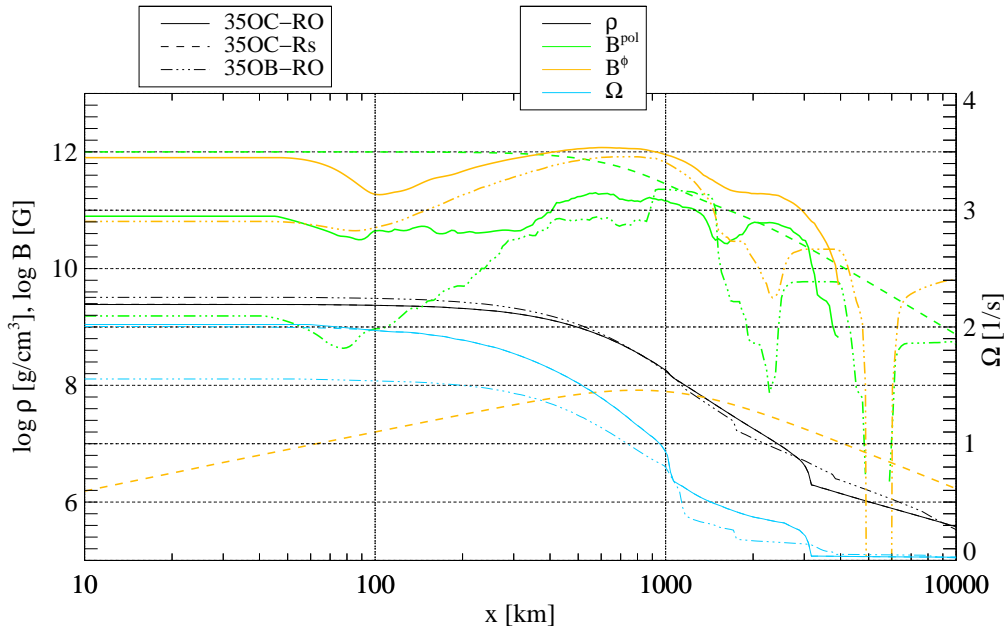


**Figure 1.** Profiles of density, angularly averaged poloidal and toroidal magnetic field, and angular velocity for all three models at the onset of collapse.

where the volume integration extends over the surface region defined above.

We first note that no crust has formed in any of the models. Hence, the dynamics of the surrounding region in which the PNS is immersed, characterized by radial as well as angular flows, leaves an imprint on the structure and evolution of the surface field. Consequently, we can find important variations of the strength and orientation of the field on intermediate length scales at all times for model 350C-RO (left panels). At  $t = 0.24$  s, regions where the poloidal field is mostly radial are situated close to ones where the  $\theta$ -component is strongest, and the toroidal field shows reversals of polarity, though on average negative/positive in the northern/southern hemisphere. These patterns are reflected in rather strong currents localized in domains of an angular extent around  $\lesssim 20$  degrees. These general observations hold also at later times. In addition, we find an enhancement of the field strength at the north and south poles, where the PNS radius is lowest. There, the poloidal field is mostly radial. Variations on very small length scales lead to intense currents. We note that the gas ending up in the bipolar explosion is accelerated in the small volume immediately outside the polar PNS surface.

The angular spectra of the poloidal field are rather similar for all three times shown here, except for a growth of the mean field strength. Modes up to  $l \lesssim 10$  possess a similar spectral power. Going to higher orders, the spectra decay according to a power law with an index slightly exceeding 1. The spectra of the toroidal field are somewhat steeper towards low order modes with a power-law component beginning already at  $l < 10$ . In agreement with the partition of the energy between poloidal and toroidal field, the toroidal spectrum is about an order of magnitude stronger than the poloidal one.

Model 350C-Rs presents a similar case, albeit at a much higher axis ratio of the PNS and with a more equal distribution of energies of the poloidal and toroidal components. Compared to the above model, the enhancement of the radial field and the concentration of the currents at the polar caps are more pronounced. As before, the poloidal component shows a spectral plateau at  $l \lesssim 10$ , while the spectrum of the toroidal field has a power-law shape across the entire range of modes.

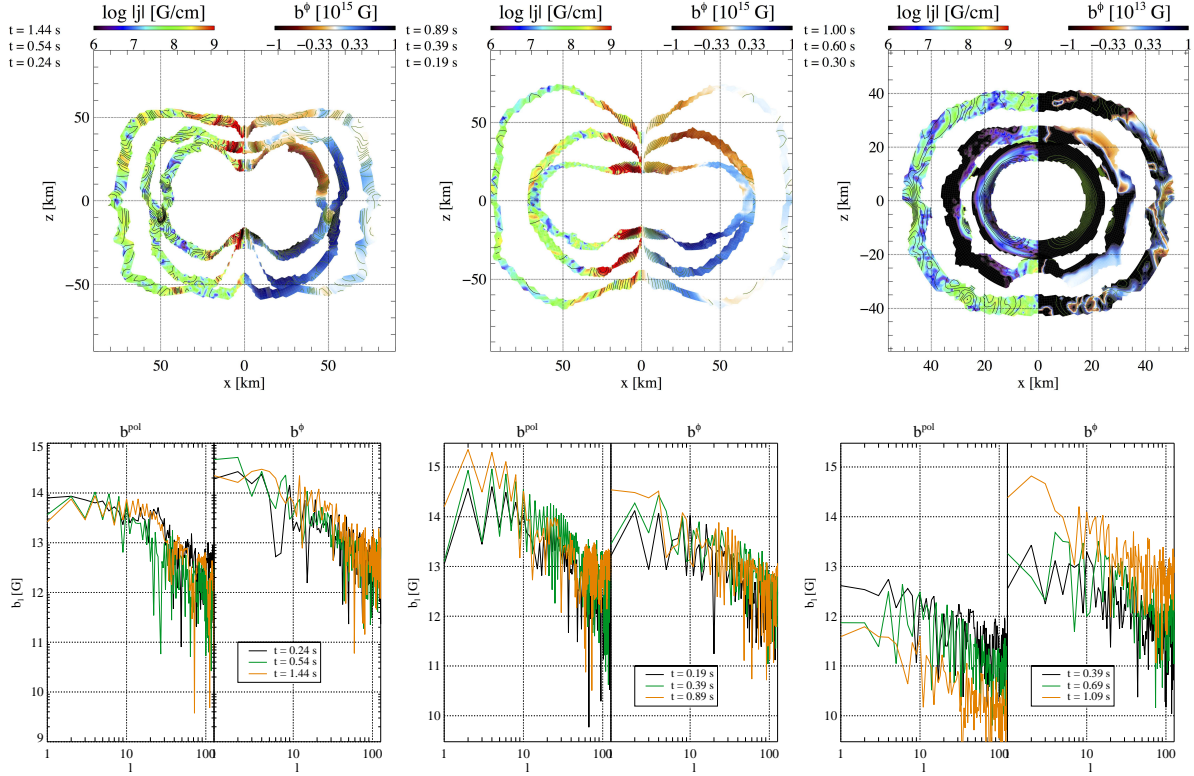


**Figure 2.** Top row: maps of the current density (colours in the left parts of the figures) and toroidal field component (right parts) overlaid by field lines of models (left to right) 350C-R0, 350C-Rs, and 350B-R0. For each model, we only show the surface layer of the PNS at three different times as printed in the top left part of the figures. Due to the contraction of the PNS, the outermost, intermediate, and innermost PNS surfaces correspond to the sequence from the earliest to the latest times. Bottom row: angular spectra of the absolute value of the poloidal and the toroidal field components of the same models at the three times shown in the top row.

The evolution of model 350B-R0 differs from this pattern mostly due to the large unmagnetized shell that is accreted onto the PNS after the iron core. At an early stage of the model ( $t = 0.39$  s), the qualitative results are similar to the other two models: variations on large and intermediate scales dominate the structure of both field components and the surface layer is filled by a highly variable pattern of currents. However, at later times, gas without a magnetic field is accreted, burying the field already present in the PNS. Therefore, the PNS surface at  $t = 0.69$  s is, except for the polar caps, almost devoid of magnetic field. At intermediate to low latitudes, poloidal field can be found only at its base. It does not reach the matter surrounding the PNS. The toroidal field is slightly less confined to the interior, but also rather weak outside the PNS. During the later phases of accretion and contraction of the PNS, this picture is modified slightly. At  $t = 1.09$  s, the structure of the field is visible to a larger extent at the bottom of the surface layer. The poloidal field lines are now entirely closed within the PNS. Even the polar region where at  $t = 0.69$  s still some radial field lines were present is no longer threaded by field lines connected to the surrounding matter. Still, the toroidal field is slightly more extended, but also drops quickly with radius. Any speculation as to whether this mostly buried magnetic field might reemerge later is idle because of the quick collapse to a BH. For this model, the plateaus in the spectra of the poloidal component tend to be even more extended than for the two models discussed above. The toroidal component, which is by far stronger than, also shows

notable power at high-order modes.

#### 4. Conclusions

We investigated the structure and evolution of the magnetic field on the surface of rapidly rotating PNSs, which are the results of the axisymmetric simulations coupling magnetohydrodynamics with a spectral two-moment neutrino transport solver of [8]. We selected three representative models based on two different cores, one developing a magnetically supported explosion and leaving behind a PNS (350C-R0), one exploding very energetically driven by the magnetic field and with an extremely oblate PNS at the centre (350C-Rs), and a third one that explodes with little magnetic influence and produces a BH at the end of the simulation (350B-R0).

For each of the models, we studied the morphology of the poloidal and toroidal magnetic field components on the PNS surface, which we approximately identified with the  $\nu_e$ -sphere, at different times and computed the angular spectra of the two components by expanding their distribution in terms of spherical harmonics. We typically find a rather complex field geometry with field lines tangled on small to intermediate length scales. An enhancement of the field strength at the polar caps of the PNSs is particularly prominent for models 350C-R0 and 350C-Rs. For both models, the surface fields are quite strong, reaching or exceeding  $10^{14}$  G on average, which would correspond to magnetars when placed in the parameter space of old neutron stars. The angular spectra of the field can be described in terms of a combination of a plateau at low mode orders,  $l$ , and a power-law decay towards higher  $l$ . The former component is most clearly visible for the poloidal component, for which it extends to  $l \gtrsim 10$ , whereas the toroidal component shows only slight hints of its presence at lowest  $l$ . This behaviour means that the field cannot be described well in terms of a single low-order mode such as, e.g. a dipole. Model 350B-R0 possesses a similar field early on, but later undergoes a transition to a very weakly magnetized surface as the magnetic field is buried underneath unmagnetized gas accreted at late times. The spectra of the field shows the same two components, but on a much weaker strength compared to the other two models strength.

We attribute this field structure to two main agents governing the field evolution: the internal dynamics of the PNS and the accretion of matter with a varying degree of magnetization. The PNSs develop convective activity quickly after their formation. While the surface usually is not part of the convective layer, it is nevertheless affected by overshoot from below. Convective eddies typically have sizes up to intermediate angles of few tens of degrees, which are reflected in the strength of the spectra at these angles. The field embedded in the gas falling onto the PNS surface is modulated by the non-radial flows in the post-shock layer on angular scales similar to those of the motions inside the PNS. At late times, after the onset of the explosions, these accretion flows take the shape of relatively narrow streams with an angular width that also corresponds to intermediate orders  $l \sim 10$  impinging on the PNS at stochastically changing locations. Hence, the effect of both processes cannot be clearly disentangled. In the absence of a magnetic field in the accreted matter, the PNS surface rather quickly turns virtually non-magnetic, despite the ongoing activity of magneto-convection below. This fact suggests that accretion rather than the PNS convection is the process mainly responsible for generating and maintaining the surface field.

The main limitations of the current study, both caused by the restrictions of computational time, are the assumption of axisymmetry and the still fairly limited simulation time. The latter restriction prevents us from studying, e.g. the possible reemergence of buried magnetic fields in cores obtaining a similar structure to model 350B-R0. To remedy both drawbacks at the same time is currently not feasible. Shorter three-dimensional runs, on the other hand, can be done at reasonable costs, albeit not for a large number of models. Running the simulations until the crust formation would be desirable since the field evolution on the surface is slowed down

considerably after that moment. So far, such a long simulation time of about 70 s has been achieved by [13] in spherical symmetry. To reach comparable times in axisymmetry, we would have to drastically reduce the computational costs by replacing the full neutrino transport by a much simpler treatment at a suitably chosen moment. Otherwise, computational costs range in several millions of core-hours per model. This problem is exacerbated by the fact that the main factor driving up the costs is the not the grid size, but the large number of time steps, against which parallelization does not offer a straightforward solution.

### Acknowledgements

We acknowledge support from the European Research Council (grant CAMAP-259276) and from the Spanish Ministry of Economy and Finance and the Valencian Community grants under grants AYA2015-66899-C2-1-P and PROMETEOII/2014-069, resp. We thank Oliver Just and Thomas Janka for valuable help, in particular regarding the aspects of microphysics and neutrinos. The computations were performed under grants AECT-2016-1-0008, AECT-2016-2-0012, AECT-2016-3-0005, AECT-2017-1-0013, and AECT-2017-2-0006 of the Spanish Supercomputing Network on hosts *Pirineus* of the Consorci de Serveis Universitaris de Catalunya (CSUC), *Picasso* of the Universidad de Málaga, *FinisTerrae2* of the Centro de Supercomputación de Galicia, Santiago de Compostela, and *MareNostrum* of the Barcelona Supercomputing Centre, respectively, and on the clusters *Tirant* and *Lluisvives* of the Servei d'Informàtica of the University of Valencia.

### References

- [1] G. S. Bisnovaty-Kogan and S. G. Moiseenko. *Progress of Theoretical Physics Supplement*, 172:145–155, 2008.
- [2] A. Burrows, L. Dessart, E. Livne, C. D. Ott, and J. Murphy. *ApJ*, 664:416–434, #jul# 2007.
- [3] S. Harikae, T. Takiwaki, and K. Kotake. *ApJ*, 704:354–371, #oct# 2009.
- [4] O. Just, M. Obergaulinger, and H.-T. Janka. *MNRAS*, 453:3386–3413, November 2015.
- [5] V. M. Kaspi. *Proceedings of the National Academy of Science*, 107:7147–7152, #apr# 2010.
- [6] P. Mösta, C. D. Ott, D. Radice, L. F. Roberts, E. Schnetter, and R. Haas. *Nature*, 528:376–379, December 2015.
- [7] P. Mösta, S. Richers, C. D. Ott, R. Haas, A. L. Piro, K. Boydston, E. Abdikamalov, C. Reisswig, and E. Schnetter. *ApJL*, 785:L29, #apr# 2014.
- [8] M. Obergaulinger and M. Á. Aloy. *MNRAS*, 469:L43–L47, July 2017.
- [9] M. Obergaulinger, H.-T. Janka, and M. A. Aloy. *MNRAS*, 445:3169–3199, December 2014.
- [10] E. O’Connor and C. D. Ott. *ApJ*, 730:70, #apr# 2011.
- [11] H. Sawai, S. Yamada, and H. Suzuki. *ApJL*, 770:L19, #jun# 2013.
- [12] H. C. Spruit. *A&A*, 381:923–932, #jan# 2002.
- [13] Y. Suwa. *Publications of the ASJ*, 66:L1, April 2014.
- [14] Y. Suwa, T. Takiwaki, K. Kotake, and K. Sato. *Publications of the ASJ*, 59:771–785, #aug# 2007.
- [15] T. Takiwaki, K. Kotake, and K. Sato. *ApJ*, 691:1360–1379, #feb# 2009.
- [16] A. Torres-Forné, P. Cerdá-Durán, J. A. Pons, and J. A. Font. *MNRAS*, 456:3813–3826, March 2016.
- [17] C. Winteler, R. Käppeli, A. Perego, A. Arcones, N. Vasset, N. Nishimura, M. Liebendörfer, and F.-K. Thielemann. *ApJL*, 750:L22, #may# 2012.
- [18] S. E. Woosley and A. Heger. *ApJ*, 637:914–921, February 2006.